JOURNAL OF SOLID STATE CHEMISTRY 20, 287–295 (1977)

The Fe–Se System. II. Mössbauer Diffusional Line-Broadening Studies of $Fe_{1+x}Se_2$ ($x \sim 0.5$, i.e., $Fe_{\sim 3}Se_4$)

TOSHIHIDE TSUJI,* ARTHUR T. HOWE, AND NORMAN N. GREENWOOD†

Department of Inorganic and Structural Chemistry, University of Leeds, Leeds LS2 9JT, England

Received August 30, 1976

Diffusional line broadening of the ^{57}Fe Mössbauer resonance has been observed in samples of $Fe_{1+x}Se_2$ ($x = 0.50$ and 0.55) in the temperature range 820 to 980°K. The lineshapes could not be fitted to a single Lorentzian peak and indicated non-Lorentzian behavior. The lattice, which has the NiAs–CdI_2 structure, contains jump pathways in one, two, and three dimensions, each of which is predicted to give a different line shape when the jump frequency approaches the mean life of the Mössbauer excited state (~100 nsec). The observed shapes were not consistent with only one-dimensional diffusion or only three-dimensional diffusion, but could be interpreted as arising from a mixture of several of the jump types.

It has recently been shown (*2*) that the diffusion of Fe in $Fe_{1.33}Te_2(Fe_2Te_3)$ is sufficiently rapid at 900°K to allow the observation of Mössbauer line broadening. The structure adopted by this highly nonstoichiometric telluride is of the NiAs–CdI_2 type for which recent theoretical considerations have shown that information concerning the diffusion mechanism can be obtained from the shape of the broadened Mössbauer absorption (*3*). We have extended our studies to the Fe–Se phase, represented by $Fe_{1+x}Se_2$, which adopts the NiAs–CdI_2 structure from the nearly stoichiometric composition ($x \approx 1$) to approximately $Fe_{1.5}Se_2$ (*4*). In this paper we report our results for the composition region near $Fe_{1.5}Se_2$ (Fe_3Se_4). Mössbauer and electrical conductivity studies of the iron-rich phase $Fe_{1.04}Se$, which adopts the anti-PbO structure, were reported in Part I (*1*).

The normally occupied octahedral cation sites within the *hcp* anion lattice of the NiAs structure are shown in Fig. 1. In the CdI_2 structure the cations are absent from every second layer. In $Fe_{1.5}Se_2$ these alternate layers are half-filled in an ordered fashion at room temperature (*5*). Referring to Fig. 1, the central metal atom has 20 adjacent octahedral sites. It is generally recognized (*6*, *7*) that diffusion within this anisotropic structural framework could occur via three types of diffusion pathway. A one-dimensional pathway involves jumps in the *c*-axis direction only (ε-type jumping). The central atom would jump to one of the two closest sites situated directly above or below. A two-dimensional pathway involves jumps by the central metal to any of the six sites within the same horizontal layer (α-type jumping) either via a direct route or via one tetrahedral interstice (indicated by the tetrahedra in Fig. 1). A three-dimensional pathway is constituted by jumps of the central metal to any of the seven sites in the layer above, or the seven sites in the layer below, via two tetrahedral intersticies (δ-type jumping).

Values of the self-diffusion coefficients for compounds having the NiAs–CdI_2 structure

* On leave from the Faculty of Nuclear Engineering, Nagoya University, Japan.

† Author to whom correspondence should be addressed.

ISSN 0022-4596

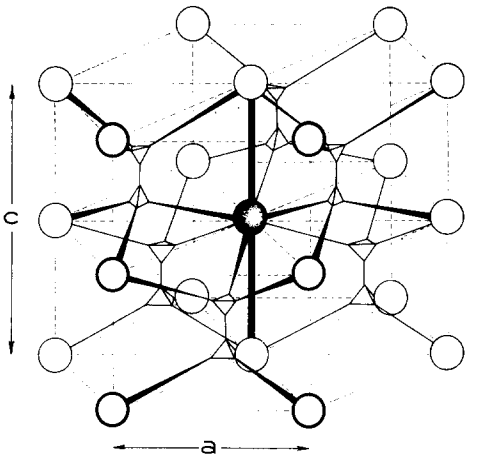

FIG. 1. Metal atom sites (circles) within the *hcp* lattice of nonmetals (not shown) in the NiAs structure. The (unoccupied) tetrahedral interstitial sites available for diffusion pathways are shown as tetrahedra.

are only known for near-stoichiometric $Ni_{1-x}S$ (*8*) and $Fe_{1-x}S$ (*6*) and have been obtained from radioactive tracer studies. In both cases diffusion in the *c* direction was slightly faster than that in the *a* direction. However, interpretation of the results in terms of the above mechanisms has been rather uncertain (*6*, *7*), and has been hindered by the difficulty in including the effects of correlation, especially in the case of one-dimensional jumping. In this case the Bardeen–Herring correlation factor could approach zero. The NiAs–CdI_2 structure can also be retained following intercalation to give compounds such as Na_xTiS_2, which has recently been investigated as a rapid ionic conductor (*9*).

The Mössbauer lineshape in the presence of diffusional broadening is sensitive to the above diffusion mechanisms (*3*, *10*). In particular the lineshape predicted from the one-dimensional jumping is characteristically different from that obtained from the other two types, and Mössbauer studies should provide a valuable probe of the jump pathways.

Experimental

The following procedure was developed in order to prepare the selenide free from traces of oxide, which, if present, reacted at high temperatures with the silica sample holder to give Fe_2SiO_4. Peaks arising from Fe_2SiO_4 were noticeable in the high-temperature Mössbauer spectra of $Fe_{1.33}Te_2$ (*2*). Spectra of the present samples showed no trace of this impurity, from which it could be deduced that the oxygen content was less than about 0.01 atom%.

Johnson Matthey specpure iron powder was reduced in purified hydrogen at 670°K for 1 day and 1270°K for 1 day. Several sintered chunks were reduced again in the same manner. Fe_2O_3 powder, having an iron isotope enrichment to approximately 90% ^{57}Fe (Harwell) was added to the Fe chunks, and reduced again in the same manner before being finally transferred under purified hydrogen to a preweighed bottle. The required quantity of prereduced (620°K for 1 day) specpure selenium was weighed out on a microbalance and the separate elements were placed in the individual arms of a W-shaped silica tube. The iron was reduced again in the same manner, and the selenium chips were then tipped into the iron section and the tube was sealed under a pressure of 13 Pa (0.1 Torr) of hydrogen. The tube was slowly heated to 870°K in an external hydrogen atmosphere, then after 1 day the sample was melted at 1350°K for 3 days, and cooled during 1 day. The tube was broken, the boule ground in an agate mortar, and the powder (approximately 200 mg) loaded into the previously degassed and hexane-filled Mössbauer sample holder. All of these operations were performed under deoxygenated hexane. The sample holder was a very-thin-walled silica cylinder about 12 mm in diameter and 3 mm in height, with a narrow loading port attached. After evaporation of the hexane, hydrogen was let in to a pressure of 13 Pa and the capsule sealed at the base of the port while the bulk of the capsule was immersed in liquid nitrogen.

X-Ray photographs of selected samples, taken on a Guinier camera, showed the monoclinic cell characteristic of the Fe_3Se_4 region (*5*). Monoclinic symmetry arises from the ordering of the cations into strings in the partly empty layers, in addition to the CdI_2-type ordering. Samples of composition $Fe_{1.55}Se_2$ and two of $Fe_{1.50}Se_2$ were studied. The

Mössbauer spectra up to 500°K both before and after the high-temperature runs were consistent with the compositions as prepared. The spectra of $Fe_{1.55}Se_2$ showed traces of the magnetically split spectrum of Fe_7Se_8 above the Néel point of Fe_3Se_4, confirming that the composition was nearly at the subphase boundary between the two regions. At higher temperatures the two subphases merge into a single-phase region (*4*). The spectra of the $Fe_{1.50}Se_2$ samples showed no trace of any other phase. The weights of the elements were accurate to within 0.1%, and were taken to define the compositions.

The capsules were placed in a boron nitride holder, together with a small amount of granulated carbon getter, inside a Ricor Mössbauer vacuum furnace controlled to within 0.2°K by a Ricor TC 4B controller with a dc furnace supply unit to eliminate ac hum. The behavior of the samples was completely reproducible even after measurements at around 970°K lasting several months. Microscopic inspection of the capsules after the high-temperature runs showed that the particles, which were not plate like in shape, had not sintered to any appreciable extent, and were still essentially randomly oriented.

Mössbauer spectra were obtained using a Goodman-type transducer driven by an Exeter-type triangular waveform generator, a 50-mCi $^{57}Co/Rh$ source, a Harwell proportional counter (methane, argon) and a Northern Scientific 900 multichannel analyzer utilizing 512 channels. The narrow pulse-height gate used to counter the scattering effects of the heavy atoms was regularly checked so that accurate area comparisons could be made. The furnace was vibrationally isolated from the pump and the floor, and the spectrum of a natural iron absorber showed no vibrational effects.

From unfolded spectra obtained at temperatures just below the onset of diffusional broadening the geometrical effect was found to be 0.06% of the total counts. Folding the spectra would result in an approximate cancellation of the opposite effects from the two sides of the triangular waveform, but would leave residual effects due, first, to second-order terms in the expression for the geometrical effect, and second, to a possibly uneven sample cross section or nonalignment effects. The absorption intensities of even the broadest peaks resulting from diffusion were still 0.2–0.3% at 973°K and were thus many times more intense than any possible lack of cancellation of the geometrical effect upon folding, thereby ensuring that folding produced essentially flat baselines. The folding point was defined by computer fits to the data over 512 channels. The isomer shifts are quoted with respect to iron foil at 295°K as zero.

Results

Figure 2 shows typical spectra obtained from $Fe_{1.55}Se_2$ and $Fe_{1.50}Se_2$ at temperatures up to 973°K. The spectrum of $Fe_{1.50}Se_2$ taken at 823°K shows no broadening effects, and at lower-velocity scans a partially resolved quadrupole doublet was evident. Below this temperature all the spectra were well behaved, and showed a slight increase in the quadrupole splitting at lower temperatures as expected. Above 823°K the resonances broadened, as can be seen from Fig. 2, until at 973°K the half-widths were several millimeters per second. The associated reduction in intensity (percentage absorption) by a factor of about 10 can be gauged by comparing the intensity scales for the spectra at successively higher temperatures. At 973°K it was necessary to count for about 6 weeks in order to achieve the desired signal-to-noise ratio.

The large reduction in intensity at the higher temperatures resulted in a peak from traces of iron in the aluminium foils becoming noticeable. Six foils constituted the heat shields of the furnace and one foil was in the counter window. A blank run was performed at 973°K without a sample but with the furnace and several silica capsules in the beam to produce a pulse-height spectrum very similar to that obtained with the sample in position. The spectrum obtained, using a low-velocity scan, could be fitted by two overlapping peaks of equal intensity having isomer shifts of −0.10 and 0.27 mm sec^{-1}, half-widths of 0.48 mm sec^{-1} and intensities of 0.11% each, giving a resultant total envelope intensity of 0.14%.

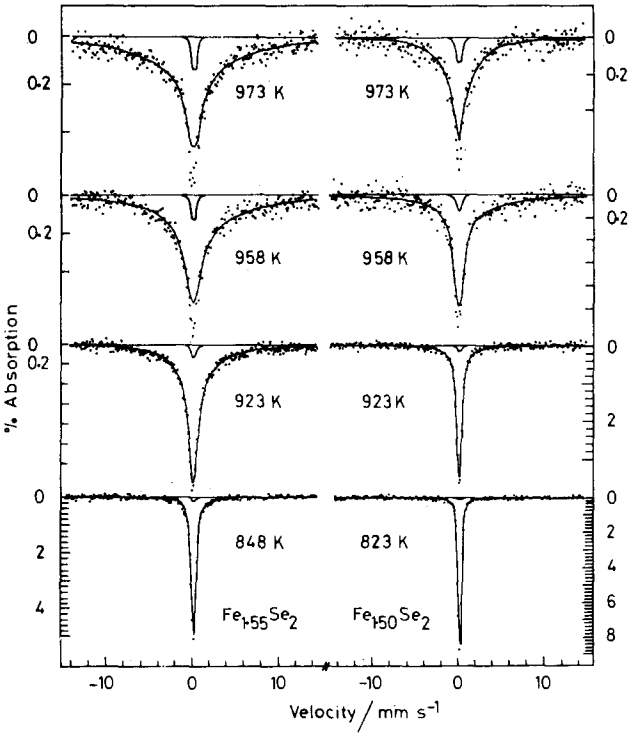

FIG. 2. High-temperature Mössbauer spectra of $Fe_{1.55}Se_2$ and $Fe_{1.50}Se_2$ showing line broadening. The experimental points represent the sum of the iron selenide spectra (solid lines) and a small peak from the furnace windows, also shown.

Since, at the highest temperatures studied, the effects of saturation on the selenide spectra would be minimal, it is safe to subtract the peaks due to Fe–Al from the observed spectra to give the true iron selenide spectra, and these resultant selenide spectra are indicated by the lines in Fig. 2. Also shown for each spectra are the two small unresolved peaks due to Fe–Al. The method of computation will now be described.

At temperatures below the onset of broadening, the data could be satisfactorily computer fitted to two unconstrained Lorentzian peaks, showing a quadrupole splitting of 0.20 mm sec^{-1} at 773°K for all samples. The half-widths of each of the doublet components were almost constant up to 773°K, and their average values are plotted in Fig. 3 for the sample of $Fe_{1.55}Se_2$.

The broadened spectra obtained at higher temperatures were initially computed as single Lorentzian peaks, with the two peaks from Fe–Al included in the fits using fixed parameters as determined from the blank run. Such fits were found to have rather high values of χ^2 for 249 degrees of freedom, as can be seen from Table I. Allowing the intensities of the Fe–Al peaks to float did not result in improved χ^2 values. As a rough guide to the general behavior, the half-widths of the single peak are shown as crosses in Fig. 3 for temperatures above 800°K.

A two-peak fit to the spectra, plus the two fixed Fe–Al peaks, resulted in acceptable values of χ^2, as can be seen from Table I. Allowing the intensities of the Fe–Al peaks to float, or even omitting the peaks completely, still resulted in acceptable fits. The solid lines shown in Fig. 2 are the sums of the two peaks obtained from a two-peak fit plus two fixed Fe–Al peaks, and thus represent an acceptable least-squares fit to the spectra of the iron selenides.

The half-widths of the two selenide peaks are shown in Fig. 3 as a function of tempera-

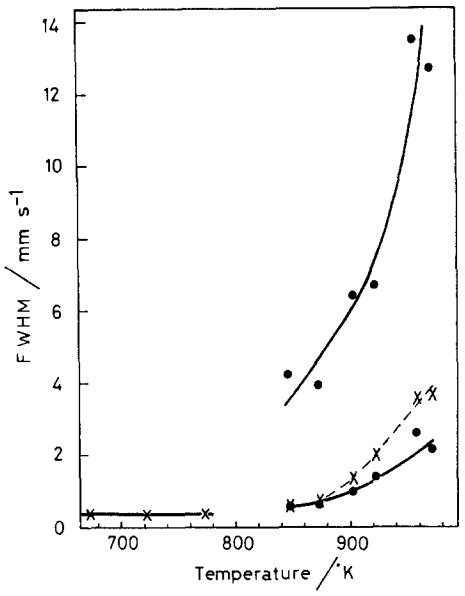

FIG. 3. Temperature dependence of the full width at half-maximum resonance of the spectrum of $Fe_{1.55}Se_2$. Above 800°K the crosses refer to a single-peak fit to the selenide spectra, and the dots to a two-peak fit.

TABLE I

χ^2 VALUES FOR ALTERNATIVE FITS TO THE SPECTRA OF $Fe_{1.55}Se_2$ WITH 249 OR 252 DEGREES OF FREEDOM, RESPECTIVELY

Temperature (°K)	χ^2 One-peak fit	χ^2 Two-peak fit
873	350	228
903	312	229
923	408	240
958	282	237
973	320	260

ture. Both peaks broaden, with the half-width of the broader peak increasing very sharply with temperature up to 13 mm sec^{-1} at 973°K. The broadening of the peaks is so much greater than the magnitude of the quadrupole splitting that this splitting would not be resolvable, and the incorporation of doublet behavior into the computer fits at the highest temperatures was not warranted.

As the temperatures of measurement are more than 200°K below the melting point, we attribute the line broadening to diffusional effects. Howe and Morgan (*3*) have predicted non-Lorentzian lineshapes for diffusional broadening in the NiAs–CdI_2 structure. The two-peak fits therefore do not represent two groups of atoms, but rather approximations (which appear to be quite good in this case) to single non-Lorentzian absorptions. As a general analytical expression for the non-Lorentzian lineshapes cannot be obtained for a polycrystalline sample containing two types of metal atoms (as in the CdI_2-type structures), we have presented the data for the two-peak fits as a guide to the trends in the broadening behavior.

The areas of the peaks are shown in Fig. 4 as a function of temperature. Up to 773°K the areas are the sums of the two components of the unbroadened quadrupole doublets. Above this temperature the individual areas of the two broadened peaks are shown, together with the total area. It can be seen that as the temperature increases so does the contribution of the broader peak to the total area. Only by taking account of these areas do the total values of the areas show the expected monotonic behavior. Knauer (*11*) showed that the area should not be affected by diffusional broadening, and the Debye–Waller temperature dependence should extend over the entire temperature range studied; this is seen to be approximately so. Up to 773°K gradual desaturation reduces the slope of the plot from that otherwise expected. At the onset of broadening some desaturation would be

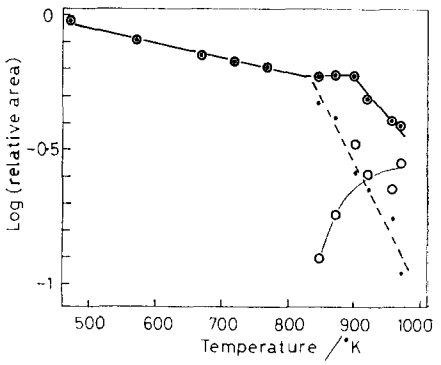

FIG. 4. The change in area as a function of temperature for the spectrum of $Fe_{1.55}Se_2$. Circled dots refer to total areas, single dots to the areas of the slightly broadened peaks, and circles to the areas of the considerably broadened peaks.

expected which would result in a small increase in the area. There are indications of this in Fig. 4, after which the normal thin-absorber slope is adopted. If no account is taken of the broader peak, or if the data obtained from one-peak fits (plus the Fe–Al peaks) are considered, the area drops off very rapidly with increasing temperature, contrary to predictions.

The behavior of the two samples of $Fe_{1.50}Se_2$ was similar to that of $Fe_{1.55}Se_2$ just described except that the onset of diffusional broadening occurred at a higher temperature. This can best be seen from a comparison of the respective spectra shown in Fig. 2. At 848°K the broadening of the spectrum of $Fe_{1.55}Se_2$ is comparable to that found at 923°K for $Fe_{1.50}Se_2$. Similarly the broadening of the spectra at 923 and 958°K for the respective samples is comparable and this is again so at 958 and 973°K. According to the phase diagram proposed on the basis of available data (*4*), an order–disorder transition occurs at about 750°K in $Fe_{1.55}Se_2$, but this rises to 977°K for $Fe_{1.50}Se_2$. The line-broadening data have thus been obtained in the disordered region for $Fe_{1.55}Se_2$, but in the ordered region for $Fe_{1.50}Se_2$. Specific heat measurements (*12*) suggest that the transition only represents the loss of order within each partly empty layer while retaining the alternately filled layers of the CdI_2-type structure. High-temperature crystallographic data are unavailable.

In the discussion we are concerned with the dependence of the shape of the Mössbauer absorption on the jump type, which has been shown (*3*) to be virtually independent of the state of order within the lattice, and indeed of the unit cell parameters (*10*). On the other hand, calculation of the diffusion coefficients from the Mössbauer data would require a knowledge of both of these factors.

Discussion

In the presence of diffusional line broadening in the NiAs–CdI_2 structure, the Mössbauer absorption cross section is given by (*3*)

$$\sigma_a(E) = \frac{\sigma_0 \Gamma \pi}{2\hbar} \exp(-2W_a)\{S_1(\mathbf{k}\omega) + S_2(\mathbf{k}\omega)\}.$$

In this expression Γ is the experimental linewidth at half-maximum height in the absence of broadening; W_a is the Debye–Waller factor; and

$$S_1 = \frac{N_1}{2\pi(N_1 + N_2)} \times \left\{ \frac{\omega^2\left(\frac{\Gamma}{\hbar} + X_1 + X_2\right) - \left(\frac{\Gamma}{2\hbar} + X_2 + Y_2\right)\left(\omega^2 + Y_1 Y_2 - \left(\frac{\Gamma}{2\hbar} + X_1\right)\left(\frac{\Gamma}{2\hbar} + X_2\right)\right)}{\omega^2\left(\frac{\Gamma}{\hbar} + X_1 + X_2\right)^2 + \left(\omega^2 + Y_1 Y_2 - \left(\frac{\Gamma}{2\hbar} + X_1\right)\left(\frac{\Gamma}{2\hbar} + X_2\right)\right)^2} \right\}.$$

S_2 is obtained by interchanging N_1 and N_2, X_1 and X_2, and Y_1 and Y_2 in S_1. Further,

$$X_1 = \alpha(1 - N_1)\,(6 - f(\mathbf{k})) + 2(\varepsilon_2 + 9\delta_2)\,(1 - N_2),$$

$$Y_1 = 2\cos\left(\frac{\mathbf{k}\cdot\mathbf{c}}{2}\right)((\varepsilon_1 + 3\delta_1) \times (1 - N_1) + \delta_1(1 - N_1) f(\mathbf{k})),$$

and X_2 and Y_2 are obtained from X_1 and Y_1 by interchaning the subscripts 1 and 2. In these last expressions $f(\mathbf{k}) = \sum_{nn}\cos(\mathbf{k}\cdot\mathbf{r}_{nn})$ i.e., the sum over the nearest neighbors.

ε_1 (1D jumping) and δ_1 (3D jumping) are the intrinsic jump rates onto partly empty layers (of average site occupancy N_1). ε_2 and δ_2 describe jumps on to almost filled layers (of average occupancy N_2). α (2D jumping) has been taken to be the same for both layers, and the expected small effect of ordering within the a planes has not been considered.

The spectra for polycrystalline samples were calculated by averaging over all solid angles. The lattice parameters for $Fe_{1.5}Se_2$ ($a = 355$ pm, $c = 558.5$ pm at room temperature) (*5*) were used. The simulated spectra were rather insensitive to small changes in the lattice parameters such as might occur with temperature or composition effects. One-dimensional jumping resulted in highly cusped peaks, two-dimensional jumping gave less cusped peaks,

while for three-dimensional jumping the shape approached Lorentzian behavior. Karyagin (*10*) demonstrated a similar behavior for different structures and pointed out that the lineshapes were characteristic of the different dimensionalities, almost independent of the particular lattice.

Differences in the shapes of the simulated peaks can be quantified by plotting the intensities versus the full width at half-maximum (fwhm). This has been done, using a log–log scale, in Fig. 5 for each type of jumping. The curves represent changes in the intensities and fwhm as the jump frequencies increase, resulting in lower intensities and larger fwhm at the bottom of the graph. The curves represent spectra all having the same area. For ease of comparison with the experimental data the intensities have been normalized to fractions of the intensity obtained in the absence of diffusional broadening. The top of the graph is thus for zero broadening, and a value of the fwhm of 0.484 mm sec^{-1} has been adopted for the simulated spectra so as to coincide with that obtained from the experimental points.

The spectra were simulated over a range of jump frequencies (in the region of 10^7 to 10^9 Hz) for both the disordered situation ($N_1 = N_2$) and an ordered situation (taken to be for $N_1 = 0.56$, $N_2 = 0.99$). Only slight differences were found for these two cases, and the hatching in Fig. 5 links the two curves obtained for each jump type. The curves at lower values of the fwhm are for the ordered situation, as certainly expected for $Fe_{1.50}Se_2$.

Lorentzian behavior is described by the straight line as shown, a consequence of the simple inverse relationship between intensity and fwhm at constant area. Jumping of the δ-type (3D) results in a lineshape very close to Lorentzian. Comparing the fwhm at a given intensity reveals the slightly cusped nature of the peak in the presence of α-type (2D) jumping, and the very markedly cusped peak obtained in the presence of ε-type (1-D) jumping. These shapes are compared in Fig. 6, where the thin lines represent the simulated peaks and the heavy line represents an experi-

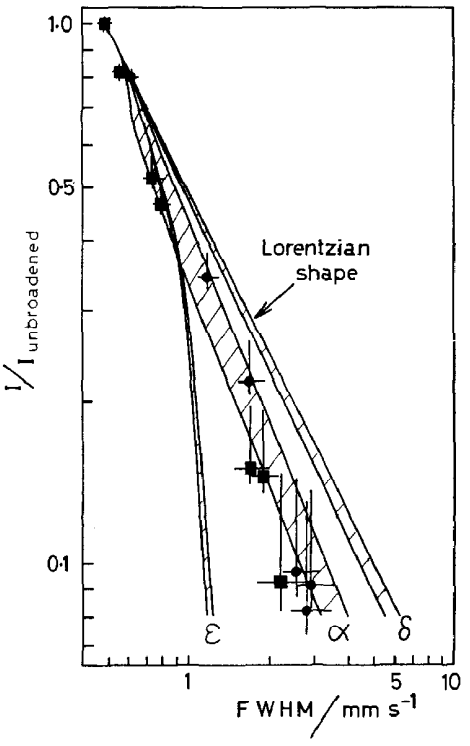

FIG. 5. Comparison of the shapes of the simulated spectra for the three different jump pathways. The intensity, I, as a fraction of the intensity of an unbroadened peak, is plotted against the full width at half-maximum (fwhm), and the values are compared to Lorentzian behavior. The squares represent the experimental data for $Fe_{1.50}Se_2$. The circles represent the experimental data for $Fe_{1.55}Se_2$.

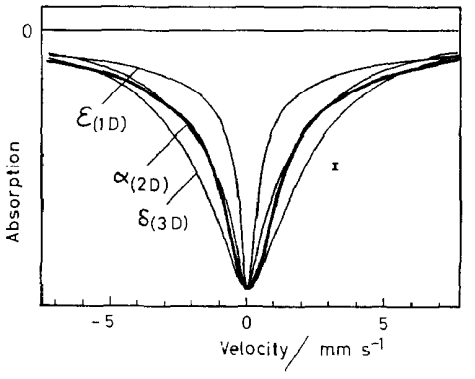

FIG. 6. Simulated spectra for the three-jump pathways, which have the same intensity ratio as the experimental spectrum of $Fe_{1.55}Se_2$ at 973°K. The least-squares fit to the experimental data of this spectrum is shown as the heavy line. The standard deviation of the scatter of the counts of the experimental spectrum is indicated.

mental shape. We shall now compare the experimental results with the above predictions.

In order to place experimental points on the plot of intensity versus fwhm, the sum of the intensities of the two selenide peaks, as obtained from the computer fits, was expressed as a fraction of the intensity of the spectral envelope at 773°K. The values were increased to correct for the normal reduction in the response at higher temperatures. The correction factor was determined from the areas obtained at 773°K, divided by the area at high temperature, obtained by a straight-line extrapolation of the data. The effect of desaturation would be to increase the values of the intensity ratios, and an estimate of this effect, using the actual areas obtained at high temperatures, is reflected in the error bars reaching to larger ratios in Fig. 5, where the experimental points are plotted. A specific correction for desaturation was, however, felt to be unwarranted in view of the errors present from other sources, particularly those of a statistical nature. The fwhm were measured from the computer-drawn fits to the data, showing the sums of the two Lorentzian peaks, which were taken to be good least-squares fits to the non-Lorentzian shapes.

Data for both $Fe_{1.55}Se_2$ and $Fe_{1.50}Se_2$ are shown in Fig. 5, and it can be seen that the points fall in the region between the two extremes represented by δ- and ε-type jumping. Such a conclusion is also evident from a visual comparison of the peak shapes. In Fig. 6 simulated peaks for the three types of jumping are shown. Each peak has the same intensity ratio as that of the experimental data of $Fe_{1.55}Se_2$ at 973°K, for which the least-squares fit (sum of the two Lorentzians) is shown. The increase in the values of the fwhm from ε- to α- to δ-type jumping, as indicated in Fig. 5, is clearly evident. The experimental shape is again seen to be between the two extremes of ε- and δ-type jumping. For almost the entire peak the difference between the experimental curve and that for ε-type jumping alone is considerably larger than the standard deviation of the statistical scatter of the spectra.

The results allow the following conclusions to be drawn regarding the diffusion pathways.

(i) The peak shapes obtained are not consistent with the presence of ε-type jumping alone.

(ii) The data are not consistent with the presence of δ-type jumping alone. This is most convincingly shown by the inability of the data to be fitted to a single Lorentzian peak, and is supported by the data given in the plot of intensity versus fwhm.

(iii) The data are consistent with (but do not necessarily require) α-type jumping only. Such a result would imply a large energy difference between the nearly filled and partly empty layers in the ordered arrangement. On the other hand there is no evidence for such anisotropic diffusion in $Fe_{1-x}S$ (*6*) and $Ni_{1-x}S$ (*8*), although the structures are disordered at the temperatures of measurement.

(iv) The most likely interpretation is a mixed-pathway process, involving both ε- and δ-type pathways or α, ε, and δ pathways in such a way as to produce the observed intermediate line shapes.

Expressions for the diffusion coefficients in terms of the jump frequencies for the general case of cation order within the lattice have been given by Howe and Morgan (*3*). In the present case where several pathways may be operating simultaneously accurate values cannot be derived for the jump frequencies, and hence for the diffusion coefficients and activation energies. However, values can be estimated for the pure ε, α, and δ pathways and the range would be expected to encompass any combination of pathways. The extent of order will also influence the diffusion coefficients. Considering these factors, the diffusion coefficients would appear to lie in the range 10^{-10} to 10^{-12} m^2 sec^{-1} at 973°K. A figure of 130 ± 60 kJ mol^{-1} was derived for the activation energies of both samples. Tracer studies on $Fe_{1-x}S$ (*6*) showed diffusion coefficients of about 10^{-12} m^2 sec^{-1} at 970°K and an activation energy of 80–90 kJ mol^{-1}, increasing up to the maximum value of x studied, 0.15. The values for the selenide are thus in a range similar to that of the sulfide. The selenide, as well as the sulfide, can therefore be described, at these temperatures, as a fast ionic conductor, a property which appears to be favored by the NiAs–CdI_2

type of lattice for transition metal chalcogenides. It is of interest to note that diffusional line broadening was also found in highly non-stoichiometric $Fe_{1-x}O$ over a temperature range similar to that of the selenide, and that the deduced activation energy was 140 ± 20 kJ mol^{-1} (*13*).

We have shown that the angular dependence of the Mössbauer line broadening can be used to identify particular diffusion pathways in an anisotropic lattice, and the technique holds great promise for the direct determination of jump displacement vectors, particularly if single crystals are measured. Such information is unobtainable using other techniques.

Acknowledgment

Financial support (to A.T.H.), from the Royal Society for the purchase of equipment, and a fellowship from the Japan Society for Promotion of Science/ Royal Society (to T.T.) are gratefully acknowledged.

References

1. T. TSUJI, A. T. HOWE, AND N. N. GREENWOOD, Part 1. *J.Solid State Chem.* **17**, 157 (1976).
2. A. T. HOWE, P. COFFIN, AND B. E. F. FENDER, *J. Phys. C: Solid State Phys.* **9**, L61 (1976).
3. A. T. HOWE AND G. J. MORGAN, *J. Phys. C: Solid State Phys.* **9**, 4463 (1976).
4. S. R. SVENDSEN, *Acta Chem. Scand.* **26**, 3757 (1972).
5. A. OKAZAKI AND K. HIRAKAWA, *J. Phys. Soc. Japan* **11**, 930 (1956).
6. R. H. CONDIT, R. R. HOBBINS, AND C. E. BIRCHENALL, *Oxid. Metals* **8**, 409 (1974).
7. G. E. MURCH, J. M. ROLLS, AND H. J. DE BRUIN, *Philos. Mag.* **29**, 337 (1974).
8. S. M. KLOTSMAN, A. N. TIMOFEYEV AND I. SH. TRAKHTENBERG, *Fiz. Metal.* **17**, 132 (1964). (*Phys. Metals Metallogr.* **17**, 119 (1964)).
9. B. G. SILBERNAGEL AND M. S. WHITTINGHAM, *Mater. Res. Bull.* **11**, 29 (1976).
10. S. V. KARYAGIN, *Phys. Lett.* **49A**, 183 (1975), *Fiz. Tverd. Tela* **17**, 1856 (1975). (*Sov. Phys. Solid State* **17**, 1220 (1975)).
11. R. C. KNAUER, *Phys. Rev. B* **3**, 567 (1971).
12. F. GRØNVOLD, *Acta Chem. Scand.* **22**, 1219 (1968).
13. N. N. GREENWOOD AND A. T. HOWE, *J. Chem. Soc. Dalton*, 122 (1972); "Proceedings of the Seventh International Symposium on the Reactivity of Solids" (J. S. Anderson, F. S. Stone, and L. M. Roberts, Eds.), p. 240, Chapman and Hall, London, 1972.